
Investigating Adversarial Vulnerability and Implicit Bias through Frequency Analysis

Lorenzo Basile¹

Nikos Karantzas²

Alberto D’Onofrio¹

Luca Bortolussi¹

Alex Rodriguez^{1,3,*}

Fabio Anselmi^{1,4,*}

¹University of Trieste, Trieste, Italy

²Baylor College of Medicine, Houston TX, USA

³ICTP, Trieste, Italy

⁴MIT, Cambridge MA, USA

*Equal advising

Abstract

Despite their impressive performance in classification tasks, neural networks are known to be vulnerable to adversarial attacks, subtle perturbations of the input data designed to deceive the model. In this work, we investigate the relation between these perturbations and the implicit bias of neural networks trained with gradient-based algorithms. To this end, we analyse the network’s implicit bias through the lens of the Fourier transform. Specifically, we identify the minimal and most critical frequencies necessary for accurate classification or misclassification respectively for each input image and its adversarially perturbed version, and uncover the correlation among those. To this end, among other methods, we use a newly introduced technique capable of detecting non-linear correlations between high-dimensional datasets. Our results provide empirical evidence that the network bias in Fourier space and the target frequencies of adversarial attacks are highly correlated and suggest new potential strategies for adversarial defence.

1 Introduction

Regardless of their overparameterisation, deep neural networks can avoid over-fitting and generalise well to new data. This surprising property has been attributed to the so-called implicit bias of the network, which refers to the ability of the gradient to converge to solutions with good generalisation properties among the many that correctly label the training data [1, 2, 3]. Understanding this bias has been the focus of extensive research in recent years. However, it remains unclear how it leads to generalisation in non-linear complex neural networks. Indeed, with the exception of simple models [4], a formal characterisation of the implicit bias of a neural network remains a formidable challenge.

Besides generalisation, another important (and related) property of neural networks is robustness, i.e. their ability to maintain performance and accuracy when exposed to noise in input data and adversarial attacks. In particular, adversarial attacks have gained significant attention since the work of [5], as they consist of perturbations of the input that are imperceptible to humans but can drastically alter the response of a trained network. Although substantial research has been conducted to understand

Correspondence to: fabio.anselmi@units.it and alejandro.rodriguezgarcia@units.it.

Code is available at <https://github.com/lorenzobasile/ImplicitBiasAdversarial>

this vulnerability [6, 7, 8, 9, 10] and numerous strategies have been developed to mitigate its effects [11, 12, 13, 14, 15], a definitive explanation of its origins remains elusive.

In this work, we explore the relationship between two crucial properties of a trained network: its vulnerability to adversarial attacks and its implicit bias. While this problem has been the focus of recent studies, explicit results have so far only been achieved for simple networks [16, 17, 18]. In this context, the research presented in [19] is particularly valuable since it offers an algorithm to investigate a specific aspect of implicit bias, even in complex networks. Their approach highlights the *essential* input frequencies required to maintain the accuracy of a trained network. In particular, these frequencies are computed by training a learnable modulatory mask for each input image, which filters the image’s frequency content and reduce it to the bare minimum needed to maintain the correct classification. These masks act as a fingerprint for the network’s implicit bias in Fourier space since they highlight the frequencies the network depends on when processing inputs. In this work, we adapt the methodology from [19] to investigate, for each input image, the correlation between the frequencies essential for the correct classification of the image and those targeted by adversarial attacks for its misclassification. Fig. 1 displays examples of clean and attacked images before (A, B) and after (C, D) being filtered by, respectively, essential frequency masks and adversarial frequency masks. Our primary objective is to provide empirical proof that the network bias is highly correlated with the adversarial attacks in Fourier space. However, defining and computing this correlation is challenging due to the high-dimensional nature of the modulatory mask sets and their potential highly non-linear correlation. To address these challenges, we use different correlation estimators among which a recently introduced non-linear one [20] relying on the observation that the intrinsic dimensionality (I_d) of a dataset is closely linked to the correlations among the various features defining the data points. The idea is that these correlations determine the allowed regions where the data points live, effectively shaping the underlying manifold and its intrinsic dimensionality. Our findings indicate a strong correlation between the manifolds of the feature spaces defined by the two types of masks, providing empirical evidence of the connection between the network bias in Fourier space and the target frequencies of adversarial attacks.

The main contributions of this work can be summarised as follows:

- We provide the first detailed quantitative computation of the essential frequencies in adversarially attacked images.
- We demonstrate a strong correlation between implicit bias and adversarial perturbations between the essential frequencies, identified as in the first contribution, of clean and adversarial images.
- We show that the essential frequencies required to classify images in a certain class are sufficient to counteract adversarial attacks, suggesting a promising approach for designing new defense protocols.

2 Related work and background

2.1 Implicit Bias, Implicit Fourier Bias and Robustness

Overparameterised networks are characterised by a loss landscape with numerous local minima that correctly label the training data. The idea behind the phenomenon of implicit bias is that which local minimum the model converges to after training depends on the complex interplay between different factors including the choice of the architecture [4, 24], the weights initialisation scheme [25], the optimisation algorithm [26, 27] and the data statistics [28].

The implicit bias of state-of-the-art models has been shown to play a critical role in the generalisation properties of deep neural networks [1, 3]. Research over the years has thoroughly investigated the implicit bias present in training algorithms for different network architectures. Although an explicit characterisation of the bias has been found only in simple networks such as linear [29, 30, 27, 31, 32], and some nonlinear models [33, 34, 35, 17, 36, 37, 38], the phenomenon is still lacking a final explanation. Interestingly, a study by Frei et al. [17] demonstrates that the implicit bias in neural networks acts as a "Double-Edged Sword": while it enhances generalisation properties, it can also compromise the network’s robustness, presenting both benefits and potential drawbacks. Similar conclusions are reached in [39]. Conversely, [40] reveals a deep connection between robust

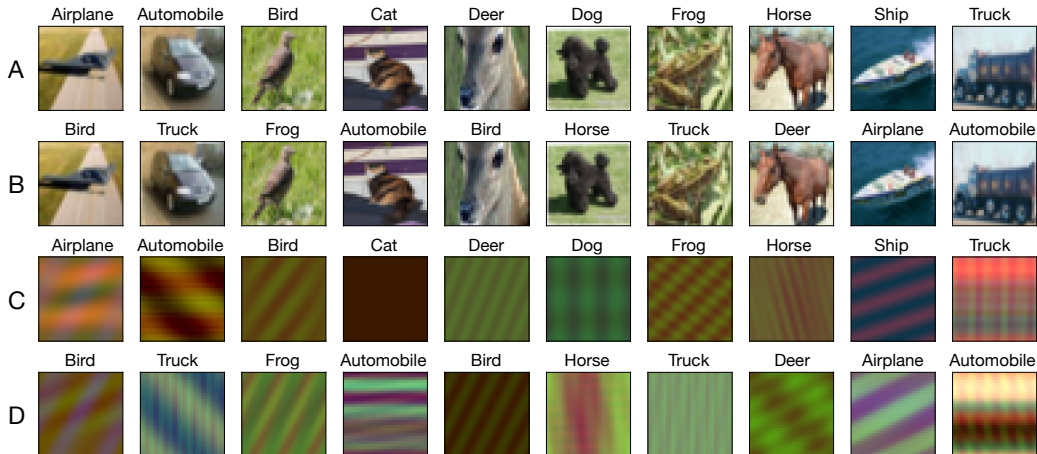


Figure 1: Examples of CIFAR-10 [21] images before and after being filtered by the Fourier masks: (A): original input images (B): adversarial images generated with ℓ_∞ Fast Minimum Norm [22] attack on ResNet-20 [23] (C): images filtered by essential frequency masks (D): adversarial images filtered by adversarial frequency masks.

classification and implicit bias, suggesting that the implicit bias can improve robustness in linear regression. Finally, in [41] the authors show that a shallow network with a polynomial ReLU activation trained by gradient flow not only generalises well but is also robust to adversarial attacks. These studies highlight that, while some insight into the relationship between implicit bias and the robustness of a neural network has been gained, a clear understanding is still lacking. One interesting effect of the implicit bias in neural networks is their tendency to learn specific frequencies in the *target function* during training, a phenomenon known as spectral bias [42]. This bias leads the network to learn low-complexity functions, potentially explaining its ability to generalise [43, 44, 45, 46]. Additionally, the implicit bias can also significantly influence the types of input features extracted by a trained neural network. For instance, [19] demonstrates that very few image frequencies in the Fourier domain are enough for the network to perform classification. These findings have helped characterise the spectral bias of neural networks with a focus on the input space rather than the target function (as in [42]). Moreover, empirical evidence shows a strong relationship between network robustness and the statistics of the Fourier spectra of the input data [28] or architecture [47]. Detection strategies in the Fourier domain have also been used to defend against adversarial attacks [48].

2.2 Adversarial attacks

Artificial Neural Networks are well known to be vulnerable to adversarial attacks [5, 6]. These attacks involve manipulating an input data point in a way that deceives an otherwise well-performing classifier, by making small alterations to a correctly classified data point. Numerous techniques have been proposed to create such adversarial examples, beginning with the Fast Gradient Sign Method (FGSM) [6], followed shortly by variants such as Projected Gradient Descent (PGD) [13]. Both these methods employ gradient information to generate an appropriate adversarial example while ensuring that the ℓ_p norm of the perturbation remains below a fixed threshold ϵ . These algorithms were primarily developed for effectiveness rather than optimality, which may limit their ability to generate input samples with minimal perturbations, resulting in them being classified as "maximum confidence" attacks. In contrast, "minimum norm" attacks prioritise the identification of adversarial examples with the least amount of perturbation by minimising its norm. In this regard, some of the most notable proposals are L-BFGS [5], the Carlini and Wagner attack [49], DeepFool [50] and the more recent Fast Minimum Norm (FMN) attack [22], which seeks to combine the efficiency of FGSM and PGD with optimality in terms of perturbation norm.

The robustness of neural networks against adversarial attacks remains an unresolved issue. Although adversarial training is currently the most effective technique for improving the resilience of neural classifiers, it often involves a trade-off between robustness and a reduction in performance on non-adversarial, clean data [6, 51]. Moreover, it remains unclear why adversarial examples exist and whether they represent an inevitable byproduct of current neural architectures and training methods [9, 52]. The goal of this work is not to propose a method for improving the adversarial robustness of neural networks. Rather, our aim is to provide valuable insights into the frequency content that is targeted by adversarial attacks and its relationship with the implicit spectral bias of the network.

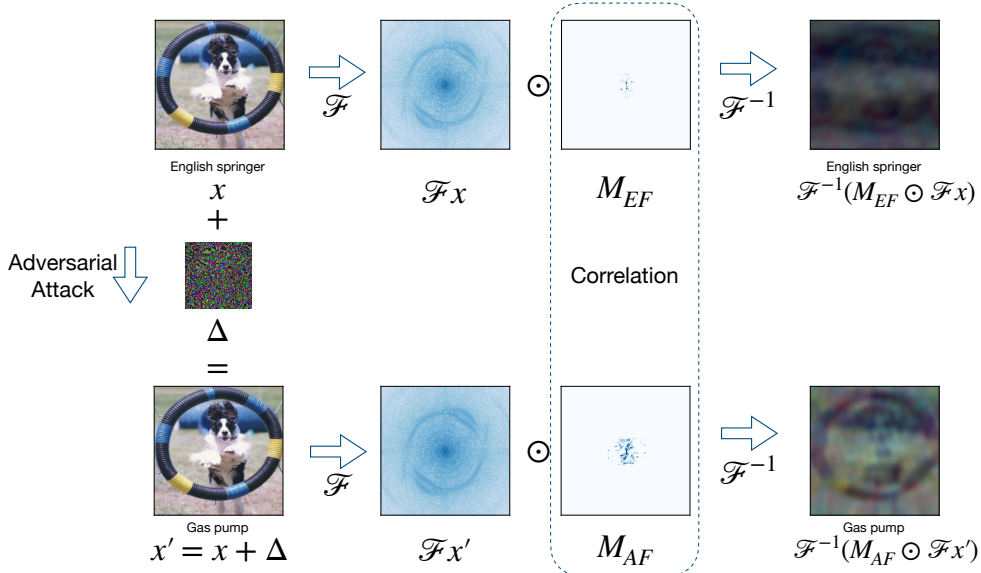


Figure 2: Schematic representation of the method employed to obtain essential frequency masks and adversarial frequency masks. Only one channel is displayed for visualization purposes. Full details are provided in Sec. 4.4.

3 Methods

3.1 Modulatory Masks

Our main tools for understanding the implicit spectral bias and the geometry of adversarial examples are modulatory masks. These masks are computed to extract information about the essential input frequencies that the network requires to perform a specific classification task. To generate these masks, we employ an algorithm similar to the one described in [19], as illustrated in Fig. 2. We train masks to modulate the frequency content of an image by performing element-wise multiplication between each entry of the Fast Fourier Transform (FFT) of the image and the corresponding entry of the mask. Each entry of the mask is a learnable scalar between 0 and 1. Specifically, starting from an image x , we compute its FFT $\mathcal{F}x$ and multiply it element-wise with a learnable mask M . The mask has the same shape of the image x (and its FFT $\mathcal{F}x$), meaning that if the image has RGB encoding we train a separate mask for each channel, and its entries are constrained to be in $[0, 1]$. The result of this multiplication is then projected back in pixel space by taking the real part of its inverse Fourier transform, thereby obtaining a new filtered image x_F :

$$x_F = \Re(\mathcal{F}^{-1}(M \odot \mathcal{F}x)). \quad (1)$$

The image x_F is then fed into the trained classification model to obtain a prediction. We produce two sets of masks. The masks belonging to the first set encode the essential frequencies of an image to be correctly classified by the neural classifier, thus we will refer to these as *essential frequency masks* (M_{EF}). The second set is composed of masks that encode the essential frequency content

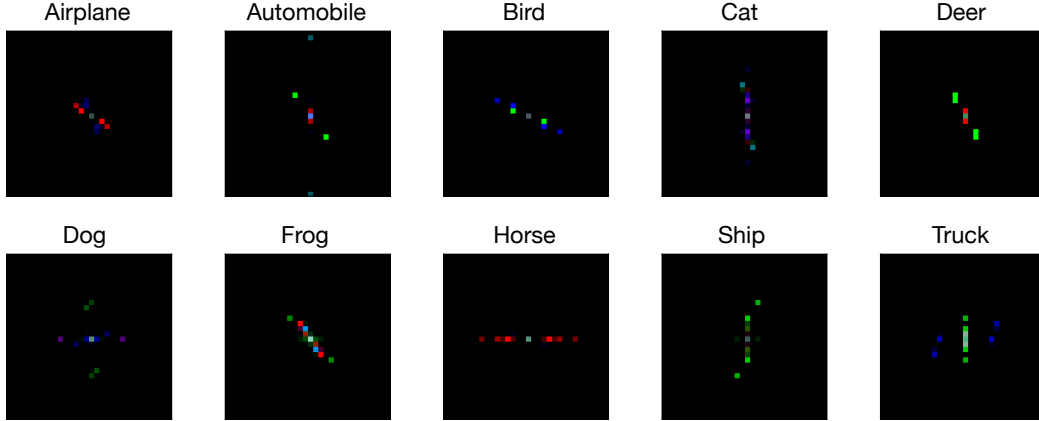


Figure 3: Examples of adversarial frequency masks, represented as RGB images. The labels refer to the classification of the clean image. The masks were obtained using CIFAR-10 and the Fast Minimum Norm attack on ResNet-20.

required to maintain the effectiveness of an adversarial attack, that is, the essential frequencies needed to misclassify an adversarially perturbed image. We will refer to these masks as *adversarial frequency masks* (M_{AF}). Some examples of adversarial frequency masks are shown in Fig. 3 (the corresponding M_{EF} masks are shown in the Appendix in Fig. 5). Both sets of masks are learned using a preprocessing layer attached to a trained ANN with frozen parameters. The essential frequency masks are trained by optimising the Cross-Entropy loss of the entire model (consisting of the preprocessing layer and the trained classifier) on the original samples. Conversely, for adversarial frequency masks, the training objective is the Cross-Entropy with respect to the adversarial class (to preserve misclassification), and the masks are trained on adversarial data.

The key property of the learned masks is their *sparsity*, which is achieved by enforcing an ℓ_1 norm regularisation on the entries of the mask during training. This regularisation ensures that the mask accurately captures only the essential frequency content needed to accomplish a specific task, such as correctly classifying an input or misclassifying an adversarial example. Our primary objective is to determine whether a correlation exists between these distinct sets of masks.

3.2 High-dimensional correlation

As mentioned earlier, to examine the statistical relationship between implicit bias and adversarial attacks, we compute the correlations between two feature spaces: that of the essential frequencies for image classification and that of the essential frequencies required for the adversarial attack to be successful. In this section we introduce the main tools that we employ to this aim. One of the most common approach for investigating correlations is based on the Pearson correlation coefficient (R^2) between variables. However, this method can only be applied to univariate datasets, making it impractical when dealing with multidimensional data, like in our case. The direct analogous to R^2 in a multivariate scenario is Canonical Correlation Analysis (CCA) [53].

CCA works by linearly projecting the two multidimensional datasets to a subspace where the correlation between the projected variables is maximised. A more modern derivative of CCA is Singular Value CCA (SVCCA) [54], which employs Principal Component Analysis before CCA, with the objective of denoising and reducing the dimensionality of data. SVCCA proved to be particularly useful in analysing the internal representations of neural networks [54]. In this direction, other correlation metrics have been proposed, including Projection Weighted CCA [55], Centered Kernel Alignment [56] and the recent Intrinsic Dimension Correlation ($I_d\text{Cor}$) [20].

$I_d\text{Cor}$ is a method for quantifying correlation that is well suited for non-linear multidimensional spaces. It is based on the concept of Intrinsic Dimension (I_d) of data, which refers to the minimum number of variables required to describe a dataset. The key idea behind $I_d\text{Cor}$ is that if there is a correlation between two datasets (i.e., the information from one can partially reconstruct the other),

the combined I_d of the datasets will be lower than the sum of their individual I_d s. This method provides both a correlation coefficient and a P-value, obtained through a permutation test, indicating the probability of no correlation.

Finally, Cosine Similarity is another method for measuring similarity between high-dimensional vectors, defined as the cosine of the angle between two vectors. Unlike other methods, cosine similarity is not strictly a measure of correlation. It offers a localized measure of similarity for individual pairs of vectors rather than evaluating entire datasets (i.e., multiple samples of a random variable). Additionally, cosine similarity requires that both vectors exist in the same vector space, making it unsuitable for vectors with different dimensionalities.

4 Experimental results

4.1 Data

For our experiments, we employed two benchmark image datasets: CIFAR-10 [21] and Imagenette [57]. CIFAR-10 consists of 60000 RGB 32×32 training images and 10000 test images categorised into 10 classes. When studying adversarial examples, we used the test images, and the training set was solely employed for fine-tuning models, as explained in greater detail in the subsequent section. Imagenette, a 10-class subset of ImageNet [58] was used to scale up our experiments to a higher-dimensional data set. In this case, images were resized to 224×224 and both training and test images (respectively, 9469 and 3925 images) were used to train modulatory masks, as detailed in Sec. 4.5.2.

4.2 Models

To gain a more complete picture of how implicit bias and adversarial attacks are related in various scenarios, we employed classification models based on different neural architectures. For CIFAR-10 data, we used ResNet-20, a relatively small representative of the very well known ResNet family, introduced in [23]. We trained the model from scratch, and provide details on the training procedure in the Appendix (Sec. A.2). In the case of Imagenette, we employed both a CNN (ResNet-18 [23]) and a Vision Transformer (ViT-B/16 [59]). We took these models pretrained on ImageNet-1K and we only trained the final classification head, to adapt it to the classification task at hand.

4.3 Attacks

We employed three ℓ_∞ gradient-based adversarial attacks: the Fast Minimum Norm (FMN) attack [22], Projected Gradient Descent (PGD) [13] and DeepFool [50]. All the attacks were employed in the untargeted setting. While FMN and DeepFool do not depend on any hyperparameter, for PGD it is necessary to allocate a perturbation budget ϵ . For most experiments, we set it to the standard value of $\epsilon = \frac{8}{255}$ [60], but we provide an analysis of the robustness of our findings with respect to ϵ in Sec. 4.6. To implement all attack algorithms, we utilized the implementation provided in the Foolbox library [61, 62].

4.4 Mask training

The key step in our experimental procedure is the training of Fourier masks (see Sec. 3.1). Starting from a trained, well-performing classifier, we freeze its parameters and prepend to it a pre-processing layer that computes the FFT of an image, multiplies it element-wise by the trainable mask and computes the inverse FFT. The real part of the resulting image is then fed into the classifier. The process of training the masks is identical for both the set of essential frequency masks and adversarial frequency masks, with the only difference being the data set used for mask training. We train essential frequency masks using clean images associated with their original labels. In contrast, for adversarial frequency masks, we utilize adversarial images and the adversarial labels produced by the classifier for those images. In this step, we optimize the standard Cross-Entropy loss function with the addition of an ℓ_1 penalty term to promote mask sparsity. Further details on the mask training procedure are reported in Sec. A.3 in the Appendix.

Table 1: Correlation between essential frequency masks and adversarial frequency masks (CIFAR-10, ResNet-20). (**SVCCA**): SVCCA [54] correlation coefficient between essential and adversarial frequency masks; (**Cosine sim**) mean \pm std. dev. cosine similarity between masks; (**I_d Cor**) correlation coefficient between masks, according to I_d Cor [20]; (**P-value**) P-value for I_d Cor (low means high probability of correlation)

Attack	SVCCA	Cosine sim	I_d Cor	P-value
FMN	0.25	0.49 ± 0.27	0.66	0.01
PGD	0.30	0.49 ± 0.28	0.60	0.01
DeepFool	0.25	0.48 ± 0.27	0.62	0.01

4.5 Correlation between adversarial and essential frequency masks

4.5.1 CIFAR-10

To provide evidence of the relation between the implicit bias of the network and the adversarial perturbations, we adopt a direct approach: we correlate the essential frequency masks with the adversarial frequency masks. This correlation analysis is performed using various methods, introduced in Sec. 3.2. Namely, we employ SVCCA [54] as a linear baseline, Cosine Similarity, and Intrinsic Dimension Correlation (I_d Cor [20]).

Correlation results for ResNet-20 on CIFAR-10 data, reported in Table 1, show that there is a clear correlation between the essential frequencies of the classifier and those of adversarial attacks. While linear correlation, measured by SVCCA, is not strikingly high, I_d Cor finds consistent evidence of correlation, as witnessed by the correlation scores above 0.6 for all attacks and high confidence (P-value = 0.01). Interestingly, even a very simple metric such as cosine similarity finds strong similarities between the two sets of masks, as average similarity is just below 0.5 for all attacks. However, cosine similarity is a local measure, returning one value for each pair of masks, and high average similarity comes at the cost of extremely high fluctuations among individual data points.

Summing up, these results point to a strong correlation between the essential and adversarial frequencies of the classifier. This correlation has a significant nonlinear component, as witnessed by the advantage shown by I_d Cor with respect to SVCCA. Moreover, its nature is strongly impacted by the individual features of images (as shown by high variations in cosine similarities).

4.5.2 Imagenette

We now move to a larger-scale experiment using Imagenette [57], a 10-class subset of ImageNet [58]. The training of modulatory masks (essential frequency masks and adversarial frequency masks) was conducted following the same procedure used for CIFAR-10, with the only difference being that both the training and test images were used to calculate the masks. This choice was made due to the reduced size of Imagenette’s test set, which could impact the accuracy of subsequent analyses. Indeed an accurate estimation of intrinsic dimension is crucial when using I_d Cor [20] as the number of data points needed for reliable estimation scales exponentially with the intrinsic dimension itself [63]. For Imagenette, we compute the same correlation statistics as provided for CIFAR-10 (SVCCA, I_d Cor, and cosine similarities). However, due to the high resolution of masks (three channels of size 224×224), repeated intrinsic dimension estimations are computationally infeasible on raw data. Therefore, we average-pool masks to 32×32 pixels before applying correlation methods. The results are reported in Table 2. Similar to the previous dataset, the discrepancy between I_d Cor and SVCCA reveals the presence of a nonlinear correlation. Correlation is found for all combinations of adversarial attack (FMN, PGD, and DeepFool) and model architecture (ResNet and ViT).

4.6 Correlation with variable perturbation magnitude

The PGD attack algorithm allows to tune the parameter ϵ , which controls the magnitude of the adversarial perturbation in terms of ℓ_∞ norm. Throughout the paper, we kept this value fixed at $\frac{8}{255}$. However, varying this parameter can provide useful insight into our results in terms of correlation between essential frequency masks and adversarial frequency masks. Interestingly, as shown in Table

Table 2: Correlation between essential frequency masks and adversarial frequency masks (Imagenette).

Attack	Model	SVCCA	Cosine sim	$I_d\text{Cor}$	P-value
FMN	ResNet-18	0.23	0.60 ± 0.15	0.63	0.01
	ViT-B/16	0.21	0.56 ± 0.18	0.59	0.01
PGD	ResNet-18	0.19	0.60 ± 0.16	0.62	0.01
	ViT-B/16	0.23	0.53 ± 0.20	0.58	0.01
DeepFool	ResNet-18	0.23	0.59 ± 0.15	0.62	0.01
	ViT-B/16	0.22	0.53 ± 0.19	0.56	0.01

3, the correlation does not directly depend on the magnitude of the adversarial perturbation, and it emerges with high confidence even with more subtle attacks, with $\epsilon = \frac{1}{255}$ and $\epsilon = \frac{3}{255}$.

Table 3: Attack success rates and $I_d\text{Cor}$ correlation results for PGD with variable perturbation magnitude ϵ on ResNet-20.

ϵ	Attack success rate	$I_d\text{Cor}$	P-value
$\frac{1}{255}$	68.56%	0.59	0.02
$\frac{3}{255}$	99.78%	0.53	0.04
$\frac{8}{255}$	100.00%	0.60	0.01

4.7 Class-specific content in masks

Expanding upon the findings presented in [19] regarding the clustering of modulatory masks, we propose the hypothesis that masks computed on images of the same class share substantial frequency content. To validate this hypothesis, we designed a simple test.

We sample multiple random subsets containing k randomly chosen classes, with k ranging from 1 to 10. Then, we apply $I_d\text{Cor}$ to essential frequency and adversarial frequency masks belonging to that specific subset of classes. For each k , we consider the average correlation and P-value over the random subsets we sampled. As an example, for $k = 1$ at each iteration we consider one random class alone, while for $k = 10$ the subset of classes we are considering is not random at all, and we are correlating the masks for all images in the CIFAR-10 dataset.

If masks belonging to the same class shared common frequencies, we would anticipate the average correlation to increase and the average P-value to decrease (and, consequently, correlation confidence to increase) as we added more classes. This is because $I_d\text{Cor}$ relies on a permutation test to compute the P-value and increasing the number of classes would lower the probability of matching masks belonging to the same class when they are permuted. In fact, in Fig. 4 a clear decreasing trend is visible for the correlation P-value versus k (and, conversely, an increasing trend in the correlation coefficient). This trend is present with all the attacks we tested (FMN, PGD and DeepFool), indicating that there is a considerable amount of class-specific information encoded in the masks.

Based on this observation, we envisioned the possibility of training a single mask that encodes the essential frequency content for an entire class. Such masks (one for each class, displayed in the Appendix A.5) can be obtained following the same approach used to learn essential frequency masks for single images, but training on all the images belonging to a certain class. We trained class-level masks on the training images of CIFAR-10 on ResNet-20 and observed that they effectively preserved correct classifications for the unseen test set, confirming that they capture a set of frequencies that covers those needed to classify each category. Motivated by these findings and by the strong correlation between adversarial attacks and essential frequencies, we move to evaluating whether essential frequency masks can help in the mitigation of adversarial attacks.

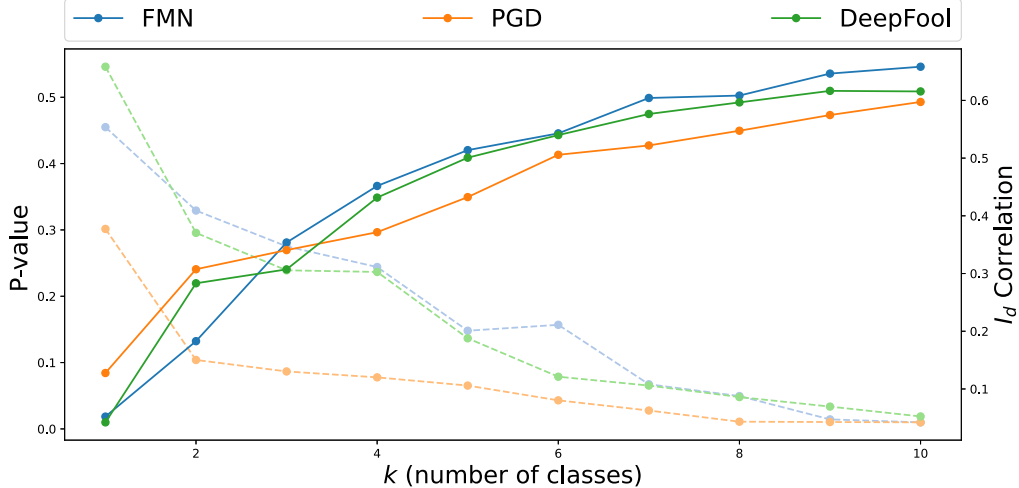


Figure 4: Average correlation according to $I_d\text{Cor}$ between k -class sets of essential frequency and adversarial frequency masks (ResNet-20). Solid lines represent correlation coefficients, while faded dashed lines represent P-values.

4.8 Modulatory masks can revert adversarial attacks

At the current point, essential frequency masks are not sufficient to counter adversarial attacks. In fact, while it is true that they encode the frequency content required to predict a certain category, prior knowledge of the correct category is needed in order to choose the right mask to apply. However, a simple modification in the mask training strategy can address this issue.

We retrain class-level essential frequency masks alternating the standard optimisation step, aimed at *preserving* correct classification of clean data, with a second step aimed at *reverting* adversarial attacks, akin to adversarial training [6]. Specifically, in this second step we consider a batch of adversarially perturbed images, all misclassified in a certain category, and optimise the mask, which we dub *robust* essential frequency mask, to revert the classification to the original category of each image.

At test time, when an unseen and potentially adversarial sample is fed to the network, the prediction can be used to pick the corresponding mask, so that a second forward pass can be executed on the filtered image. This step proves helpful in counteracting adversarial attacks (Table 4), though it imposes a toll in terms of clean accuracy, as in the case of most adversarial defence techniques [51].

Moreover, as reported in Table 4, in most cases robust essential frequency masks can generalise across different adversarial attack algorithms, meaning that exact knowledge of the type of threat one might be facing is not a crucial requirement. While this finding alone is insufficient to build a proper adversarial defence method, as an attacker may get access to the masks and produce new adversarial perturbations that deceive the masked model, we believe it represents a promising starting point for future research in this direction.

5 Discussion

Our study investigates the relationship between adversarial attacks and the implicit bias of neural networks in the Fourier domain. We focus on standard network architectures like ResNets and ViTs and datasets such as CIFAR-10 and Imagenette, where direct mathematical analysis of implicit bias is particularly challenging.

For the first time, we computed the essential frequencies required for an adversarial image to be misclassified. We demonstrated that these frequencies are highly correlated with the essential frequencies needed for a clean image to be correctly classified, using multiple correlation metrics.

Table 4: Clean and adversarial test accuracy when robust essential frequency masks are applied to ResNet-20 for CIFAR-10 classification. Rows report different adversarial attacks (including no attack, i.e. clean accuracy), while on the columns we report the results relative to masks trained on different attacks, including the base case when no mask is applied.

Data	Mask			
	None	FMN	PGD	DeepFool
Clean	0.92	0.83	0.74	0.82
FMN	0.04	0.78	0.72	0.78
PGD	0.00	0.43	0.54	0.44
DeepFool	0.00	0.77	0.71	0.78

Our work represents an advancement in understanding the nature of adversarial attacks. Identifying the crucial frequencies utilised by attackers holds promising implications for developing new defence and detection algorithms, thereby enhancing the security and robustness of neural networks. Notably, by using a variant of the essential frequency masks to revert the effects of adversarially attacked images, we showed a new direction for generating adversarial defences.

While studying the implicit bias of networks through the Fourier lens is a promising approach, that has been the focus of many recent works, it only offers a specific angle of analysis, which is a limitation of our study. However, our mask-based approach provides a flexible method for future investigations. For example, beyond examining the real part, researchers can investigate the essential Fourier phases in input images, opening new avenues for studying the implicit frequency bias of networks and their robustness. Additionally, other types of representations, such as wavelets, could be explored. Another limitation of our study is that it focuses on the input frequencies neglecting those of all the intermediate representations within the network. This area will be the subject of future investigations.

In conclusion, our framework not only enhances the understanding of adversarial attacks in neural networks but also paves the way for developing more effective defence strategies, contributing to the overall advancement of AI security.

References

- [1] Zhiyuan Li, Ruosong Wang, Dingli Yu, Simon S Du, Wei Hu, Ruslan Salakhutdinov, and Sanjeev Arora. Enhanced convolutional neural tangent kernels. *arXiv preprint arXiv:1911.00809*, 2019.
- [2] Chiyuan Zhang, Samy Bengio, Moritz Hardt, Benjamin Recht, and Oriol Vinyals. Understanding deep learning requires rethinking generalization. In *Proceedings of the International Conference on Learning Representations (ICLR), 2017*, 2017.
- [3] Sanjeev Arora, Simon S Du, Wei Hu, Zhiyuan Li, Russ R Salakhutdinov, and Ruosong Wang. On exact computation with an infinitely wide neural net. *Advances in neural information processing systems*, 32, 2019.
- [4] Suriya Gunasekar, Jason D Lee, Daniel Soudry, and Nati Srebro. Implicit bias of gradient descent on linear convolutional networks. *Advances in neural information processing systems*, 31, 2018.
- [5] Christian Szegedy, Wojciech Zaremba, Ilya Sutskever, Joan Bruna, Dumitru Erhan, Ian Goodfellow, and Rob Fergus. Intriguing properties of neural networks. *arXiv preprint arXiv:1312.6199*, 2013.
- [6] Ian J Goodfellow, Jonathon Shlens, and Christian Szegedy. Explaining and harnessing adversarial examples. In *International Conference on Learning Representations (ICLR)*, 2015.
- [7] Nicolas Papernot, Patrick McDaniel, Ian Goodfellow, Somesh Jha, Z. Berkay Celik, and Ananthram Swami. Practical black-box attacks against machine learning. In *Proceedings of the 2017 ACM on Asia conference on computer and communications security*, 2017.

- [8] Anish Athalye, Nicholas Carlini, and David Wagner. Obfuscated gradients give a false sense of security: Circumventing defenses to adversarial examples. In *International conference on machine learning (ICML)*, 2018.
- [9] Andrew Ilyas, Shibani Santurkar, Dimitris Tsipras, Logan Engstrom, Brandon Tran, and Aleksander Madry. Adversarial examples are not bugs, they are features. *Advances in neural information processing systems*, 32, 2019.
- [10] Zuxuan Wu, Ser-Nam Lim, Larry S Davis, and Tom Goldstein. Making an invisibility cloak: Real world adversarial attacks on object detectors. In *European Conference on Computer Vision (ECCV)*, 2020.
- [11] Nicolas Papernot, Patrick McDaniel, Xi Wu, Somesh Jha, and Ananthram Swami. Distillation as a defense to adversarial perturbations against deep neural networks. In *IEEE symposium on security and privacy (SP)*, 2016.
- [12] Alexey Kurakin, Ian Goodfellow, and Samy Bengio. Adversarial machine learning at scale. In *International Conference on Learning Representations (ICLR)*, 2017.
- [13] Aleksander Madry, Aleksandar Makelov, Ludwig Schmidt, Dimitris Tsipras, and Adrian Vladu. Towards deep learning models resistant to adversarial attacks. In *International Conference on Learning Representations*, 2018.
- [14] Eric Wong and Zico Kolter. Provable defenses against adversarial examples via the convex outer adversarial polytope. In *International Conference on Machine Learning (ICML)*, 2018.
- [15] Eric Wong, Leslie Rice, and J. Zico Kolter. Fast is better than free: Revisiting adversarial training. In *International Conference on Learning Representations (ICLR)*, 2020.
- [16] Spencer Frei, Gal Vardi, Peter L. Bartlett, and Nathan Srebro. Benign overfitting in linear classifiers and leaky relu networks from kkt conditions for margin maximization. *Preprint, arXiv:2303.01462*, 2023.
- [17] Spencer Frei, Gal Vardi, Peter L. Bartlett, Nathan Srebro, and Wei Hu. Implicit bias in leaky relu networks trained on high-dimensional data. In *International Conference on Learning Representations (ICLR)*, 2023.
- [18] Gal Vardi. On the implicit bias in deep-learning algorithms. *Preprint, arXiv:2208.12591*, 2022.
- [19] Nikos Karantzas, Emma Besier, Josue Ortega Caro, Xaq Pitkow, Andreas S Tolias, Ankit B Patel, and Fabio Anselmi. Understanding robustness and generalization of artificial neural networks through fourier masks. *Frontiers in Artificial Intelligence*, 5:890016, 2022.
- [20] Lorenzo Basile, Santiago Acevedo, Luca Bortolussi, Fabio Anselmi, and Alex Rodriguez. Intrinsic dimension correlation: uncovering nonlinear connections in multimodal representations. *arXiv preprint arXiv:2406.15812*, 2024.
- [21] Alex Krizhevsky. Learning multiple layers of features from tiny images. *Tech Report*, 2009.
- [22] Maura Pintor, Fabio Roli, Wieland Brendel, and Battista Biggio. Fast minimum-norm adversarial attacks through adaptive norm constraints. *Advances in Neural Information Processing Systems*, 34:20052–20062, 2021.
- [23] Kaiming He, Xiangyu Zhang, Shaoqing Ren, and Jian Sun. Deep residual learning for image recognition. In *Proceedings of the IEEE conference on computer vision and pattern recognition*, pages 770–778, 2016.
- [24] Chulhee Yun, Shankar Krishnan, and Hossein Mobahi. A unifying view on implicit bias in training linear neural networks. In *International Conference on Learning Representations*, 2020.
- [25] Justin Sahs, Ryan Pyle, Aneel Damaraju, Josue Ortega Caro, Onur Tavaslioglu, Andy Lu, Fabio Anselmi, and Ankit B Patel. Shallow univariate relu networks as splines: initialization, loss surface, hessian, and gradient flow dynamics. *Frontiers in artificial intelligence*, 5:889981, 2022.
- [26] Francis Williams, Matthew Trager, Daniele Panozzo, Claudio Silva, Denis Zorin, and Joan Bruna. Gradient dynamics of shallow univariate relu networks. *Advances in Neural Information Processing Systems*, 32, 2019.

- [27] Blake Woodworth, Suriya Gunasekar, Jason D Lee, Edward Moroshko, Pedro Savarese, Itay Golan, Daniel Soudry, and Nathan Srebro. Kernel and rich regimes in overparametrized models. In *Conference on Learning Theory*, pages 3635–3673. PMLR, 2020.
- [28] Dong Yin, Raphael Gontijo Lopes, Jon Shlens, Ekin Dogus Cubuk, and Justin Gilmer. A fourier perspective on model robustness in computer vision. *Advances in Neural Information Processing Systems*, 32, 2019.
- [29] Andrew M Saxe, James L McClelland, and Surya Ganguli. Exact solutions to the nonlinear dynamics of learning in deep linear neural network. In *International Conference on Learning Representations*, 2014.
- [30] Suriya Gunasekar, Blake Woodworth, Srinadh Bhojanapalli, Behnam Neyshabur, and Nathan Srebro. Implicit regularization in matrix factorization. In *Proceedings of the 31st International Conference on Neural Information Processing Systems*, pages 6152–6160, 2017.
- [31] Hancheng Min, Salma Tarmoun, René Vidal, and Enrique Mallada. On the explicit role of initialization on the convergence and implicit bias of overparametrized linear networks. In *Proceedings of the 38th International Conference on Machine Learning*, volume 139 of *Proceedings of Machine Learning Research*, pages 7760–7768. PMLR, 18–24 Jul 2021.
- [32] Zihan Wang and Arthur Jacot. Implicit bias of sgd in l_2 -regularized linear dnns: One-way jumps from high to low rank. *arXiv preprint arXiv:2305.16038*, 2023.
- [33] Kaifeng Lyu and Jian Li. Gradient descent maximizes the margin of homogeneous neural networks. In *International Conference on Learning Representations*, 2019.
- [34] Etienne Boursier, Loucas Pullaud-Vivien, and Nicolas Flammarion. Gradient flow dynamics of shallow relu networks for square loss and orthogonal inputs. In *Advances in Neural Information Processing Systems*, volume 35, pages 20105–20118, 2022.
- [35] Mingze Wang and Chao Ma. Understanding multi-phase optimization dynamics and rich nonlinear behaviors of reLU networks. In *Thirty-seventh Conference on Neural Information Processing Systems*, 2023.
- [36] Spencer Frei, Gal Vardi, Peter Bartlett, and Nathan Srebro. The double-edged sword of implicit bias: Generalization vs. robustness in reLU networks. In *Thirty-seventh Conference on Neural Information Processing Systems*, 2023.
- [37] Akshay Kumar and Jarvis Haupt. Directional convergence near small initializations and saddles in two-homogeneous neural networks. *arXiv preprint arXiv:2402.09226*, 2024.
- [38] Emmanuel Abbe, Samy Bengio, Enric Boix-Adsera, Etai Littwin, and Joshua Susskind. Transformers learn through gradual rank increase. *Advances in Neural Information Processing Systems*, 36, 2023.
- [39] Nikolaos Tsilivis, Natalie Frank, Nathan Srebro, and Julia Kempe. The price of implicit bias in adversarially robust generalization. *arXiv preprint arXiv:2406.04981*, 2024.
- [40] Fartash Faghri, Sven Gowal, Cristina Vasconcelos, David J Fleet, Fabian Pedregosa, and Nicolas Le Roux. Bridging the gap between adversarial robustness and optimization bias. *ICLR Workshop on Security and Safety in Machine Learning Systems*, 2021.
- [41] Hancheng Min and René Vidal. Can implicit bias imply adversarial robustness? *arXiv preprint arXiv:2405.15942*, 2024.
- [42] Nasim Rahaman, Aristide Baratin, Devansh Arpit, Felix Draxler, Min Lin, Fred Hamprecht, Yoshua Bengio, and Aaron Courville. On the spectral bias of neural networks. In *International conference on machine learning*, pages 5301–5310. PMLR, 2019.
- [43] Sara Fridovich-Keil, Raphael Gontijo Lopes, and Rebecca Roelofs. Spectral bias in practice: The role of function frequency in generalization. *Advances in Neural Information Processing Systems*, 35:7368–7382, 2022.
- [44] Yuan Cao, Zhiying Fang, Yue Wu, Ding-Xuan Zhou, and Quanquan Gu. Towards understanding the spectral bias of deep learning. In *Proceedings of the Thirtieth International Joint Conference on Artificial Intelligence*. International Joint Conferences on Artificial Intelligence Organization, 2021.
- [45] Haohan Wang, Xindi Wu, Zeyi Huang, and Eric P Xing. High-frequency component helps explain the generalization of convolutional neural networks. In *Proceedings of the IEEE/CVF conference on computer vision and pattern recognition*, pages 8684–8694, 2020.

- [46] Yusuke Tsuzuku and Issei Sato. On the structural sensitivity of deep convolutional networks to the directions of fourier basis functions. In *Proceedings of the IEEE/CVF Conference on Computer Vision and Pattern Recognition*, pages 51–60, 2019.
- [47] Josue O Caro, Yilong Ju, Ryan Pyle, Sourav Dey, Wieland Brendel, Fabio Anselmi, and Ankit B Patel. Translational symmetry in convolutions with localized kernels causes an implicit bias toward high frequency adversarial examples. *Frontiers in Computational Neuroscience*, 18:1387077, 2024.
- [48] Paula Harder, Franz-Josef Pfreundt, Margret Keuper, and Janis Keuper. Spectraldefense: Detecting adversarial attacks on cnns in the fourier domain. In *2021 International Joint Conference on Neural Networks (IJCNN)*, pages 1–8. IEEE, 2021.
- [49] Nicholas Carlini and David Wagner. Towards evaluating the robustness of neural networks. In *2017 IEEE Symposium on Security and Privacy (SP)*, pages 39–57. IEEE, 2017.
- [50] Seyed-Mohsen Moosavi-Dezfooli, Alhussein Fawzi, and Pascal Frossard. Deepfool: a simple and accurate method to fool deep neural networks. In *Proceedings of the IEEE conference on computer vision and pattern recognition*, pages 2574–2582, 2016.
- [51] Aditi Raghunathan, Sang Michael Xie, Fanny Yang, John Duchi, and Percy Liang. Understanding and mitigating the tradeoff between robustness and accuracy. In *International Conference on Machine Learning*, pages 7909–7919. PMLR, 2020.
- [52] Ali Shafahi, W Ronny Huang, Christoph Studer, Soheil Feizi, and Tom Goldstein. Are adversarial examples inevitable? In *International Conference on Learning Representations*, 2018.
- [53] H Hotelling. Relations between two sets of variates. *Biometrika*, 1936.
- [54] Maithra Raghu, Justin Gilmer, Jason Yosinski, and Jascha Sohl-Dickstein. Svcca: Singular vector canonical correlation analysis for deep learning dynamics and interpretability. *Advances in neural information processing systems*, 30, 2017.
- [55] Ari Morcos, Maithra Raghu, and Samy Bengio. Insights on representational similarity in neural networks with canonical correlation. *Advances in neural information processing systems*, 31, 2018.
- [56] Simon Kornblith, Mohammad Norouzi, Honglak Lee, and Geoffrey Hinton. Similarity of neural network representations revisited. In *International conference on machine learning*, pages 3519–3529. PMLR, 2019.
- [57] Jeremy Howard. Imagenette. <https://github.com/fastai/imagenette>, 2022.
- [58] Olga Russakovsky, Jia Deng, Hao Su, Jonathan Krause, Sanjeev Satheesh, Sean Ma, Zhiheng Huang, Andrej Karpathy, Aditya Khosla, Michael Bernstein, et al. Imagenet large scale visual recognition challenge. *International journal of computer vision*, 115:211–252, 2015.
- [59] Alexey Dosovitskiy, Lucas Beyer, Alexander Kolesnikov, Dirk Weissenborn, Xiaohua Zhai, Thomas Unterthiner, Mostafa Dehghani, Matthias Minderer, Georg Heigold, Sylvain Gelly, et al. An image is worth 16x16 words: Transformers for image recognition at scale. In *International Conference on Learning Representations*, 2020.
- [60] Francesco Croce, Maksym Andriushchenko, Vikash Sehwal, Edoardo DeBenedetti, Nicolas Flammarion, Mung Chiang, Prateek Mittal, and Matthias Hein. Robustbench: a standardized adversarial robustness benchmark. In *Thirty-fifth Conference on Neural Information Processing Systems Datasets and Benchmarks Track (Round 2)*, 2021.
- [61] Jonas Rauber, Wieland Brendel, and Matthias Bethge. Foolbox: A python toolbox to benchmark the robustness of machine learning models. *ICML Workshop on Reliable Machine Learning in the Wild*, 2017.
- [62] Jonas Rauber, Roland Zimmermann, Matthias Bethge, and Wieland Brendel. Foolbox native: Fast adversarial attacks to benchmark the robustness of machine learning models in pytorch, tensorflow, and jax. *Journal of Open Source Software* 5(5), 2020.
- [63] Jonathan Bac, Evgeny M Mirkes, Alexander N Gorban, Ivan Tyukin, and Andrei Zinovyev. Scikit-dimension: a python package for intrinsic dimension estimation. *Entropy*, 23(10):1368, 2021.

- [64] Yerlan Idelbayev. Proper ResNet implementation for CIFAR10/CIFAR100 in PyTorch. https://github.com/akamaster/pytorch_resnet_cifar10, 2021.
- [65] Diederik P Kingma and Jimmy Ba. Adam: A method for stochastic optimization. *arXiv preprint arXiv:1412.6980*, 2014.

A Appendix

A.1 Computational Resources

In terms of computational requirements, our experimental procedure encountered two major resource-intensive tasks. First, training masks necessitates individual training for each image, which consumes substantial computational resources. Second, the computation of SVCCA and repeated intrinsic dimension estimates on large, high-dimensional mask data sets poses computational challenges. Both steps can benefit from hardware acceleration and were performed on a NVIDIA A100 GPU, equipped with 40GB of RAM.

A.2 Training details and hyperparameters

As introduced in Sec. 4, we trained one model on CIFAR-10 [21] (ResNet-20 [23]) and two on Imagenette [57], namely a ResNet-18 [23] and a ViT-B/16 [59]. Here we provide additional details regarding the training (or fine-tuning) procedure of each model and the hyperparameters we chose.

Our ResNet-20 implementation was taken from [64] and it follows the original architecture the authors of [23] proposed for CIFAR-10. This model was trained from randomly initialised weights for 200 epochs, using Stochastic Gradient Descent with momentum, set to 0.9. The learning rate was initially set to 0.1, to be decayed by a factor 10 twice, after 100 and 150 epochs. ℓ_2 regularisation was employed, by means of a weight decay factor of 10^{-4} . The final accuracy on the test set of CIFAR-10 was 92.29%.

For ResNet-18 and ViT we started from pre-trained ImageNet weights. Since Imagenette has 10 classes, compared to the 1000 of ImageNet, we had to replace the classification head, and we trained that layer only while keeping the other layers frozen. We trained the models for 20 epochs using Adam [65], with a cyclic learning rate schedule, with maximum at 0.01. We achieved final test accuracies of 98.32% (ResNet-18) and 99.57% (ViT).

A.3 Details on the mask training procedure

For all the modulatory masks we produced, we employed Adam optimiser [65] with a learning rate of 0.01. According to a criterion similar to early-stopping, masks were trained until convergence, and in any case for no less than 500 optimisation steps each. We computed essential frequency masks only for correctly classified images, while adversarial frequency masks were trained exclusively for correctly classified images that were successfully made adversarial by the attack. Sparsity of masks was enforced by means of ℓ_1 regularisation, weighted by a factor $\lambda = 0.5$ for CIFAR-10 and $\lambda = 0.01$ for Imagenette.

The same setup was employed for training the class-level masks introduced in Sec. 4.7 and 4.8, with the only difference that the training procedure was conducted on batches of images belonging to each class instead of individual images. In such case, the level of sparsity to be enforced on the masks is much lower, as they need to encode a set of frequencies that covers multiple images together. λ was set to 0.01 for essential frequency masks and to 0.001 for robust essential frequency masks, as they require more fine-grained information to revert adversarial perturbations.

A.4 Examples of essential frequency masks

In Fig. 5 we provide some examples of essential frequency masks, computed on the same images employed to obtain the examples of adversarial frequency masks displayed in Fig. 3. Masks were trained starting from CIFAR-10 images on ResNet-20 architecture.

A.5 Class-level essential frequency masks

Here we display the class-level masks we obtained on the training set of CIFAR-10, using the ResNet-20 model. As mentioned in the main text (Sec. 4.7), these masks successfully capture the essential frequency content needed to correctly classify test images, unseen during the training of the masks.

Moreover, we train class-level robust essential frequency masks (Sec. 4.8), that are able to revert the effect of the adversarial attack in most cases, restoring the correct label. When applied to clean

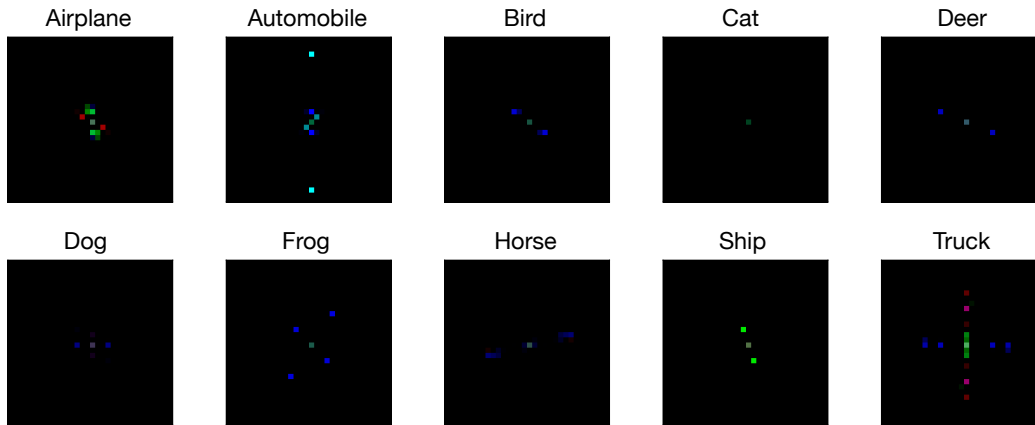


Figure 5: Examples of essential frequency masks.

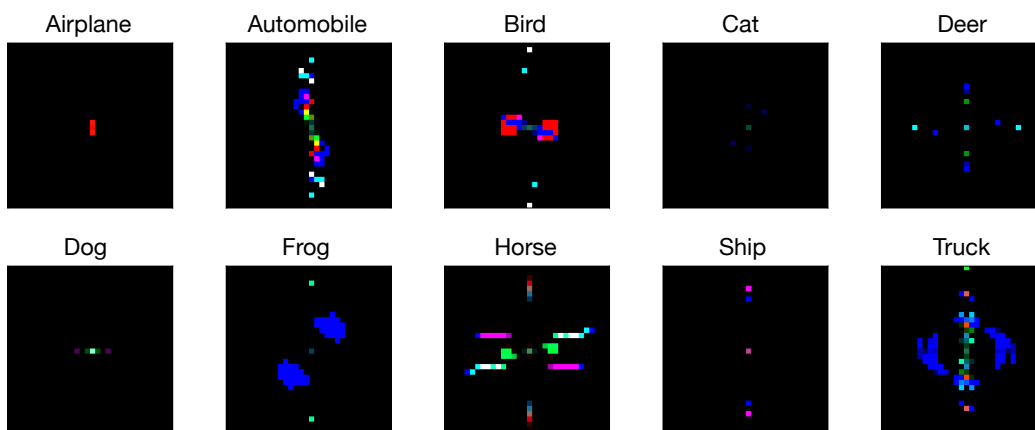


Figure 6: Class-level essential frequency masks (obtained on CIFAR-10 with ResNet-20).

data, such masks cause a slight drop in clean accuracy. Masks are trained with different sparsity requirements (regularisation λ set to 0.01 for essential frequency masks and to 0.001 for robust essential frequency masks), to account for the high-frequency bias of adversarial attacks.

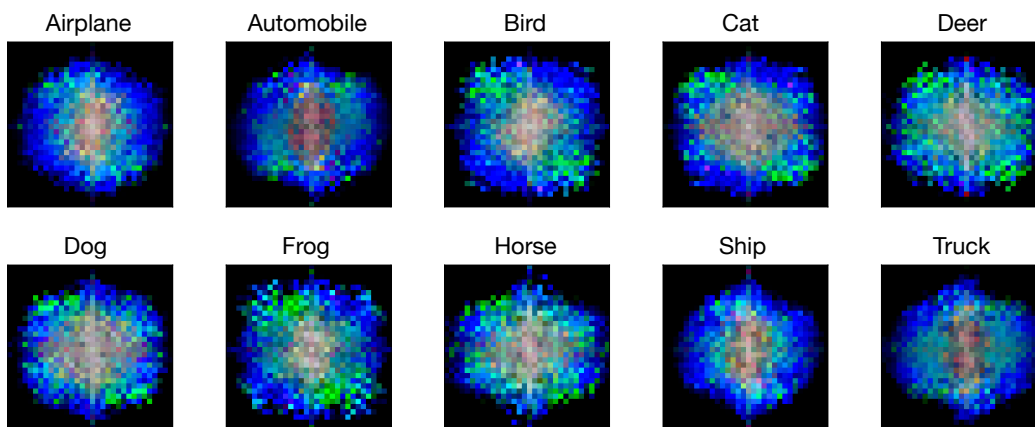


Figure 7: Class-level robust essential frequency masks (obtained on CIFAR-10 with ResNet-20, training on clean images and FMN-attacked images).